

# Analysis of Thermal Performance of Shell and Tube Heat Exchangers: A Correlation and CFD Based Approach

S.A.P Ushettige<sup>1</sup>, W.K. Wimal Siri<sup>2</sup>, H.G.S. Hikkaduwa<sup>3</sup>

<sup>1</sup>Faculty of Engineering, School of Civil and Mechanical Engineering, Curtin University,  
Bentley, WA 6102, Australia

[aperera844@gmail.com](mailto:aperera844@gmail.com) ; [walallawita.w@sliit.lk](mailto:walallawita.w@sliit.lk)

<sup>2</sup>Faculty of Engineering, Mechanical Engineering, Sri Lanka Institute of Information Technology  
Malabe, 10115, Sri Lanka

<sup>3</sup>Faculty of Engineering, General Sir John Kothalawala Defence University  
Kandawala Road, Dehiwala-Mount Lavinia, 10390, Sri Lanka  
[hikkaduwahgs@kdu.ac.lk](mailto:hikkaduwahgs@kdu.ac.lk)

## ABSTRACT

Shell and tube heat exchangers are devices which are widely adopted in thermal systems for the transfer of thermal energy due to both performance and reliability factors. Given their application in energy-intensive systems, the design and sizing of these devices have become a rapidly growing field. Traditionally, empirical correlations which were based on experimental results were used for thermal sizing and design. This was replaced by computational fluid dynamics (CFD) modelling given its ability to model and visualize flow, expanding the horizon of possibilities for design and performance optimization. Recently, CFD has been combined with numerical methods such as non-linear least-squares regression to develop correlations that predict thermal performance based on input design parameters. However, the application of this integrated method for shell and tube heat exchangers is limited. This study will model a single-pass TEMA E-type shell and tube heat exchanger using ANSYS Fluent ®. CFD simulations are used to explore the effect of turbulence on thermal performance by varying both the inlet mass flow rate and the central baffle spacing. Steady state simulations are conducted for four models with six, eight, ten, and twelve baffles. The results of CFD modelling are then combined with non-linear least squares regression in the MATLAB Curve Fitter Toolbox ® to develop four sets of correlations in the form of  $Nu = C.Re^a.Pr^b$ . Reasonably confident results were obtained in the final fitted data; however, relatively high 95% confidence interval widths were evident for certain fitted coefficients leaving space for improvement in the model. The study highlights that combining CFD with tools such as nonlinear least squares regression aids both engineers and designers in the thermal design process of shell and tube heat exchangers eliminating the need to limit design based on empirical correlations.

**KEYWORDS:** *Shell and tube heat exchangers, thermal optimization, non-linear least squares regression, central baffle spacing, turbulence, mass flow rate*

## 1 INTRODUCTION

Heat exchangers are devices commonly used to transfer thermal energy between process streams in both commercial and domestic systems (Mangrulkar et al., 2019). A range of different heat exchanger types are used in the industry. Among them, shell and tube heat exchangers are widely adopted due to their versatility in operating over, in a range of working pressures and temperatures (Sekulić & Shah, 2023). These devices also provide a large area of heat transfer for a given volume with a relatively simple construction (Pal et al., 2016; Aslam Bhutta et al., 2012). In shell and tube heat exchangers, two fluids at relatively different temperatures flow simultaneously. One flows through the tubes (tube side), and the other flows outside the tubes, or the shell, which is a circular, enclosed volume around the tubes. The energy transfer occurs through a combination of conduction and convection from the inside of the tube fluid to the outside shell fluid or vice versa (Bichkar et al., 2018). This is represented in Figure 1 (a) and (b) below.

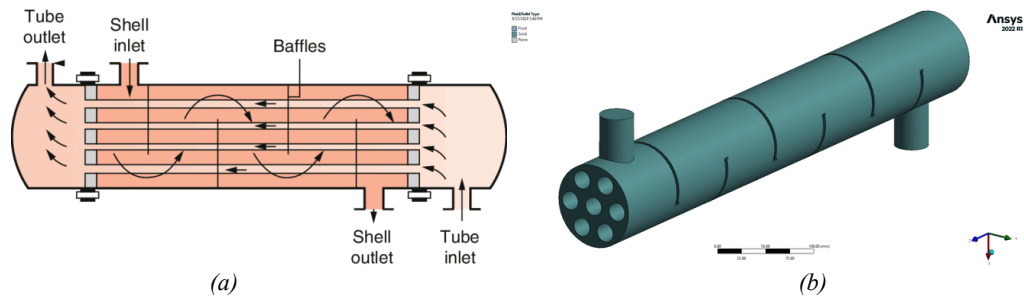


Figure 12: (a) Schematic of a Single Pass TEMA E Type shell and tube heat exchanger (M. Necati ÖZÜŞİK, 1985) (b) Physical model in ANSYS Design Modeler.

The widespread adoption of these devices in industries with significant energy transfers has made the design and sizing critical, with thermal and pressure drop as the key parameters analyzed (Huang et al., 2017). Traditionally, empirical correlations developed by organizations such as the TEMA (Tubular Exchanger Manufacturers Organization) were used. This process was time consuming and restricted design, due to the inability to visualize and identify design weaknesses in the flow (Ozden & Tari, 2010). The adoption of CFD for modelling addressed this challenge given its ability to model and visualize complex flow phenomena.

The thermo-mechanical performance in these devices depends on the level of turbulence present. This is commonly introduced using metal plates known as baffles. A range of different types and configurations can be used to achieve this (Bichkar et al., 2018). Traditionally, most models use single segmental baffles. However, the use of these types has two key drawbacks (Ozden & Tari, 2010; Pal et al., 2016; Nedunchezhiyan Mukilarasan et al., 2022; El Maakoul et al., 2016; Abbasi et al., 2020; Zhang et al., 2017). In the region present behind the baffle, “Dead zones” or areas of recirculation are created which reduce the amount of heat transfer. Additionally, the contraction and expansion effects in the fluid flow increase the pressure drop, thereby increasing the pumping power required. A common approach to optimizing performance is to adjust the configuration of baffles, the central baffle spacing and the baffle cut (Ozden and Tari, 2010; Abbasi et al., 2020). The central baffle spacing and baffle cut are identified as parameters which significantly affect the flow phenomenon and thermo-mechanical performance. Numerical work indicates that decreasing baffle spacing is associated with increased heat transfer and nozzle-to-nozzle pressure drop.

The potential of CFD design and optimization has recently been combined with tools such as non-linear least squares regression. The integration of the two tools has enabled the development of correlations that relate thermal performance to the model’s input design parameters. However, following a comprehensive survey of the existing literature, minimal applications were available for shell and tube heat exchangers. Established applications include those for a horizontal counter-flow double tube heat exchanger and plate-fin and tube heat exchanger, as reported by Alhulaifi (2024) and Marcinkowski et al. (2021), respectively. The study done by Alhulaifi (2024) explored the thermal performance of a nano-fluid flow in the device, and a correlation that predicts  $Nu$  based on  $Pr$  and  $Re$  was developed. While the study by Marcinkowski et al. (2021) involved developing a set of correlations to predict the  $Nu$  for each row based on the respective  $Pr$  and  $Re$ . A further development of the work was that done by Marcinkowski et al. (2024) which highlighted that varying the modelling scheme had minimal effect on the final outcome.

This study will use the commercial CFD solver ANSYS Fluent to model the thermal and mechanical performance of a single-pass TEMA E-type shell and tube heat exchanger. Simulations will be conducted in a steady state for the case of six, eight, ten and twelve baffles. In the effort to develop comprehensive correlations which capture the effect of turbulence on thermal performance both the central baffle spacing and the inlet mass flow rate are varied. For each model, simulations are performed over the range of 0.50 kg/s to 2.0 kg/s with increments of 0.25 kg/s. The results from the CFD analysis are then fit using non-linear least squares regression in the MATLAB Curve Fitter Toolbox to develop four sets of correlations in the form of  $Nu = C \cdot Re^a \cdot Pr^b$  where a confidence level of 95 % is used for modelling. Overall, the study is an effort to highlight the potential present in combining CFD with tools

such as non-linear least squares regressions for the design and optimization of shell and tube heat exchangers.

## 2 METHODOLOGY

### 2.1 Physical Modelling of STHX

The shell and tube heat exchangers were modelled using the ANSYS Design Modeler ® tool based on the dimensions shown in Table 1 below (Ozden & Tari, 2010). For simulation purposes, the heat transfer through the thickness of the baffles was neglected.

Table 2. Dimensions of the shell and tube heat exchanger (Ozden & Tari, 2010).

Dimensional Parameter	Value / mm
Shell Diameter	90
Outside Tube Diameter	20
Number of tubes used	7 tubes
Length of the heat exchanger	600
Central baffle spacing	86

The working fluid considered is water while, Aluminum is taken as the material for the tube walls. The presence of narrow operating temperature ranges prevented the use of piecewise linear interpolation for the properties. Additionally, simulations were done in the steady state given similar studies have utilized this assumption (Ozden and Tari, 2010; Nedunchezhiyan Mukilarasan et al., 2022; Zhang et al., 2017).

### 2.2 Computational domain, mesh and boundary conditions

The shell side volume of the four models is modelled using an unstructured tetrahedral mesh in the ANSYS Meshing tool as shown in Figure 2 below. To select the ideal mesh, a balance of accuracy and computational memory four grids were generated. The element numbers modelled were ~1.2 million, ~2.2 million, ~3.3 million and ~5.0 million. Given that the discrepancy between the overall heat transfer coefficients for the grid of 3.3 and 5.0 million was less than 2% the grid of element size 3.3 million was selected. This aligns with the level of discrepancy which has been considered reasonable in similar studies, such as that done by Abbasi et al. (2020).

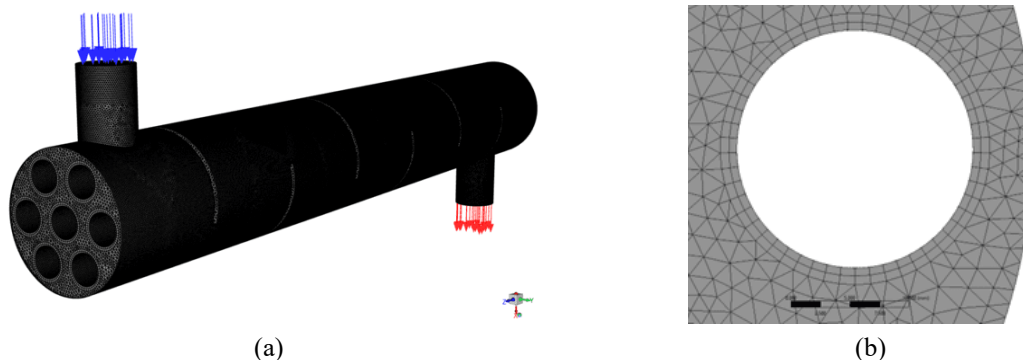


Figure 13. (a) Unstructured tetrahedral mesh with boundary conditions applied (b) Zoomed in view of the mesh applied at the tube wall.

Analysis of the contours revealed significant turbulence on the shell side of the heat exchanger. Considering merit factors such as the model's ability to capture flow detail while maintaining minimal computational time and offering simple closure, the standard  $k-\epsilon$  turbulence model was selected (Aslam Bhutta et al., 2012; Ozden and Tari, 2010; Abbasi et al., 2020). Prism layers and a scalable wall function were employed to resolve the near-wall flow in combination with the turbulence model (El Maakoul et

al., 2016; Shahril et al. 2017). This was done to limit the  $y^+ \approx 11.5$ , ensuring the flow remained compatible with the turbulence model. Control of this non-dimensional parameter which represents the distance from the wall to the first node is critical given its ability to define the near wall flow (Shahril et al., 2017). The fluid domain was defined using inlet and outlet nozzle boundary conditions. Standard mass flow and pressure boundary conditions were used respectively (Ozden and Tari, 2010, Nedunchezhiyan Mukilarasan et al., 2022; Abbasi et al., 2020; Zhang et al., 2017). Additionally, a fixed thermal condition of 450 K was used for the tube walls while a zero-heat flux condition was assumed for the shell wall.

### 2.3 Non-linear least squares regression for correlation development

The parameter formulations in the modelled correlations are similar to those used in established design methods such as the Bell-Delaware, Kern’s and flow-stream analysis methods (Jamil et al., 2020). Equations 1-3 below show the basis of calculating the  $Re$ , a similar analogy is used to evaluate both the  $Pr$  and  $Nu$  (Alperen et al., 2019).

$$D_e = \frac{4 \left( \frac{P_t}{2} * 0.87 * P_t - 0.5 * \pi * \frac{d_o^2}{4} \right)}{\pi * \frac{d_o}{2}} \tag{1}$$

$$A_s = \frac{(P_t - d_o) * D_s * B}{P_t} \tag{2}$$

$$Re = \frac{\left( \frac{\dot{m}_s}{A_s} \right) * D_e}{\mu} \tag{3}$$

## 3 RESULTS AND DISCUSSION

### 3.1 Model verification and thermo-mechanical results

Simulations revealed that increasing mass increased both the overall heat transfer coefficient and the shell side pressure drop. The results align with the trend shown in similar studies, however, differences are observed. This could be attributed to variations in the modelling schemes used. This argument is supported by the agreement visible with the study done by Pal et al. (2016) given they used a similar methodology for modelling.

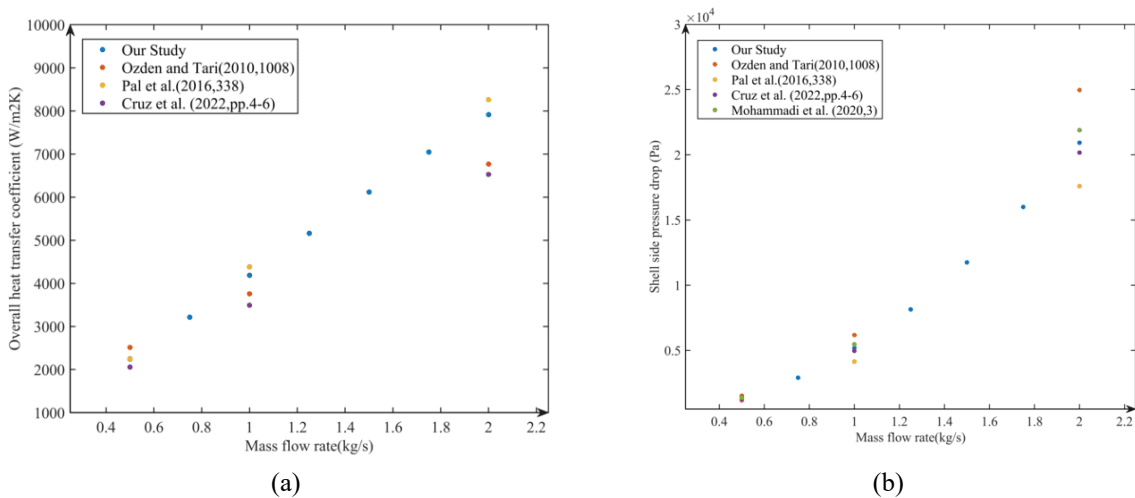


Figure 14: CFD Results for the six-baffle model (a) Overall heat transfer coefficient vs mass flow rate (b) Shell side pressure drop vs mass flow rate.

The overall heat transfer coefficient and shell side pressure were observed to be significantly affected by the increase in number of baffles and the mass flow rate as shown in Figure 4 (a) and (b) below. The overall heat transfer was observed to improve, which could be related to an improvement in the shell side flow phenomena and amount of area available for thermal transfer. Pressure drop was negatively affected, where this would lead to a higher pumping power to maintain the consistent flow of fluid. These phenomena are discussed in the context of the contours in the next section.

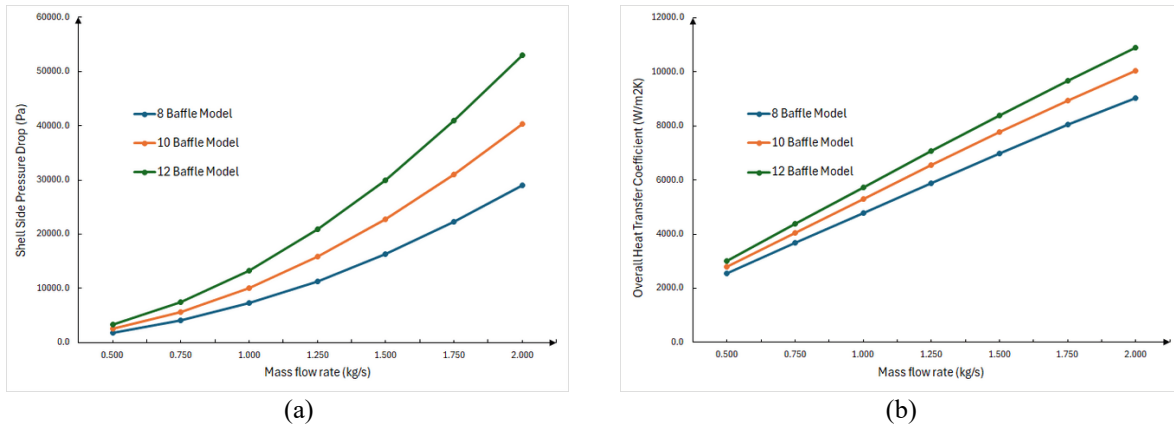
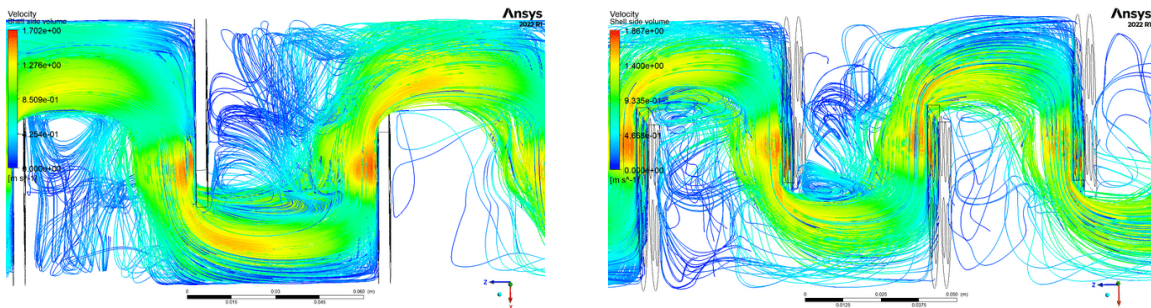


Figure 15. CFD based results with mass flow rate (a) Shell Side Pressure Drop (b) Overall Heat Transfer Coefficient

### 3.2 Pathlines

The developed pathlines reveal the fluid flow on the shell side of the heat exchanger and its dependence on the number of baffles. Fluid follows a zig-zag pattern with regions of dead zones or areas of recirculation observed behind certain baffles. The significance of recirculation areas is high at a lower number of baffles as evident in the case of 8 baffles (refer Figure 5 (a)). This is related to decreased thermal performance, as a greater amount of tube area is bypassed, thereby reducing the surface area available for heat transfer (Ozden and Tari, 2010; Alhulaifi, 2024). However, decreasing the baffle spacing was observed to improve the flow with increased flow uniformity and reduced areas of flow recirculation (refer to Figure 5 (b) and (c) below). This led to improved thermal performance as discussed earlier.



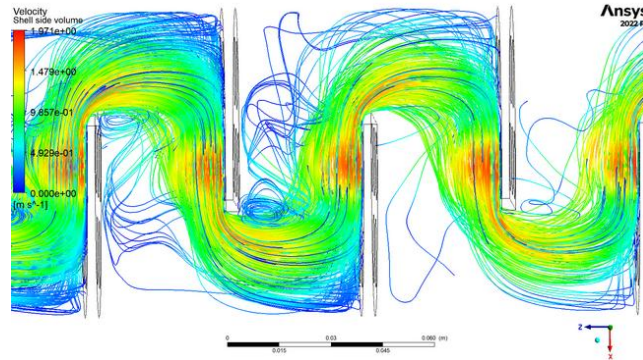


Figure 16. Velocity path lines at 1.0 kg/s (a) 8 baffles (b) 10 baffles and (c) 12 baffles.

### 3.3 Pressure drop along the length

The pressure contours reveal that the pressure drops from the inlet to the outlet along with the length of the heat exchanger. High pressure is observed at the inlet of the model due to the impingement of the fluid entering at the inlet nozzle. Flow expansion and contraction due to the presence of baffles is a key factor that introduces a significant pressure drop, as the barrier to fluid flow increases as evident in the contours. Additionally, increasing the mass flow rate is related to an increased pressure drop with relative similarity in the contours (refer Figure 6(a) – (c)).

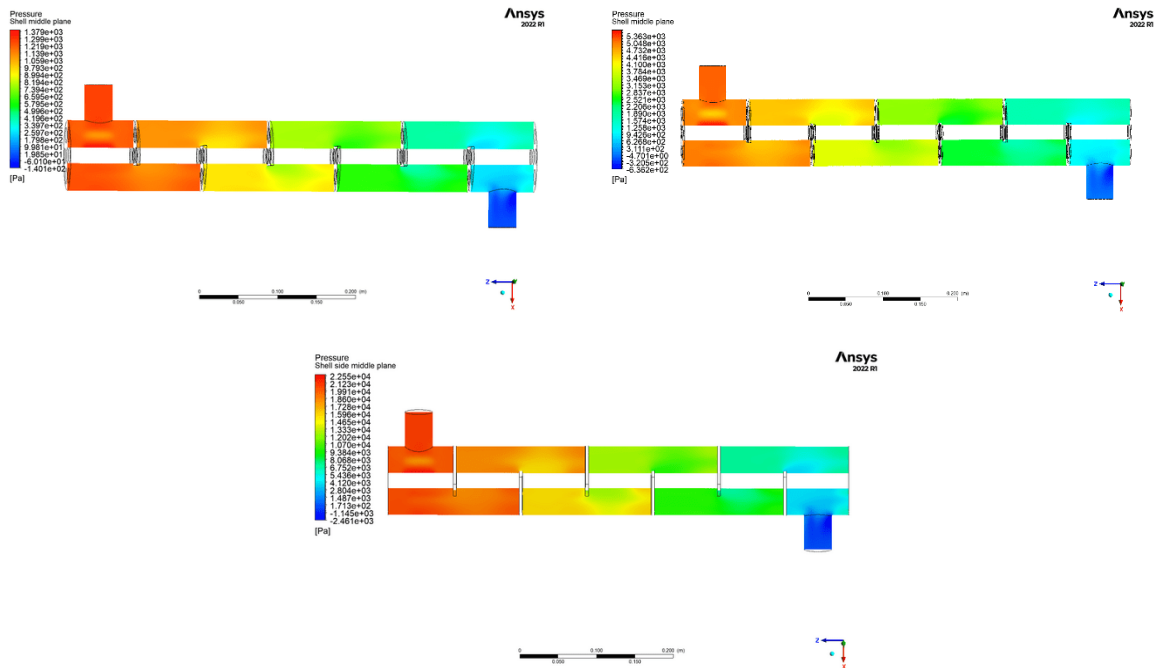


Figure 17. Pressure contours at the middle plane for six baffle model (a) 0.5 kg/s (b) 1.0 kg/s and (c) 2.0 kg/s.

Another key observation is the presence of back pressure at the outlet nozzle; this was due to improper flow development at the outlet plane. A similar observation was reported in studies by Pal et al. (2016) and Sauro & Lewis (2012).

### 3.4 CFD-Based Thermal Correlations for the four models

A summary of the correlations developed using NLSQR is shown in Figure 7 below.

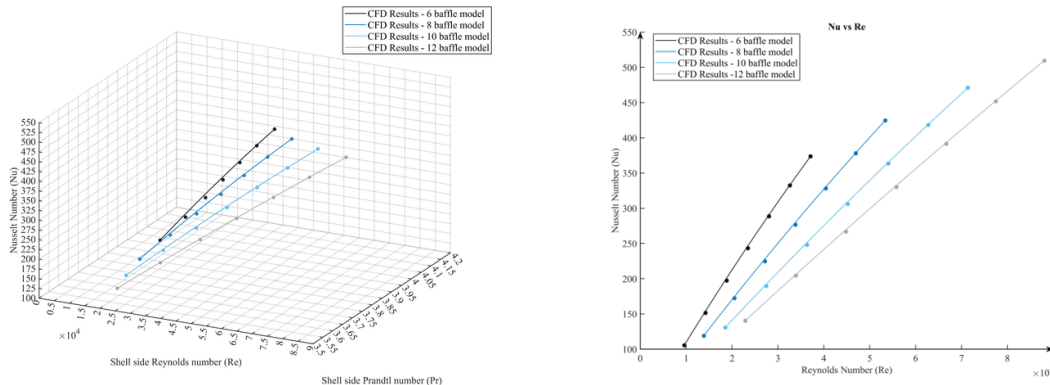


Figure 18 (a)  $Nu$  variation with  $Pr$  and  $Re$  for the four models (b)  $Nu$  variation with  $Re$  for the four models.

$Nu$  is observed to increase significantly with  $Re$ , indicative of increasing turbulence. The  $Re$  increase with both the mass flow rate and the central baffle spacing. The observed variation is a result of improved flow phenomena as revealed earlier and in similar studies done by Ozden & Tari (2010) and Abbasi et al. (2020). Additionally, the minimal variation in  $Pr$  in the observed results could be due to slight variations in the thermal properties of the working fluid. A summary of the correlations obtained using NLSQR are shown in Table 2 below.

Table 3. Summary of the correlations developed for the four models.

Baffles	$C$	$a$	$b$	$Re$ Range	$Pr$ Range
6	0.2312	0.9972	-2.1907	$9600 < Re < 37100$	$3.68 < Pr < 4.12$
8	0.139	1.0065	-2.1304	$13900 < Re < 53400$	$3.80 < Pr < 3.96$
10	0.0809	1.0103	-1.9586	$18500 < Re < 71400$	$3.66 < Pr < 3.81$
12	0.0319	0.9964	-1.2735	$22900 < Re < 88100$	$3.54 < Pr < 3.70$

The overall precision and reliability of the predicted correlations were evaluated by considering the confidence intervals (CI) widths of the predicted coefficients, a standard methodology used in numerical model evaluation (Sauro and Lewis, 2012). A summary of the upper and lower bounds of the coefficients at a 95 % confidence level is shown in Table 3 below.

Table 4. Summary of the upper and lower bounds for predicted coefficients with a 95 % confidence level.

$Nb$	6			8		
Parameter	Predicted value	Lower bound	Upper bound	Predicted value	Lower bound	Upper bound
$C$	0.2312	0.014	0.4485	0.1390	0.0158	0.2623
$a$	0.9972	0.9758	1.0186	1.0065	0.9817	1.0312
$b$	-2.1907	-3.0117	-1.3696	-2.1304	-2.9624	-1.2914
$Nb$	10			12		
Parameter	Predicted value	Lower bound	Upper bound	Predicted value	Lower bound	Upper bound
$C$	0.0809	0.0263	0.1355	0.0319	0.0207	0.0431
$a$	1.013	0.9900	1.0307	0.9964	0.9852	1.0076
$b$	-1.9586	-2.6318	-1.2854	-1.2735	-1.639	-0.908

The results show that the CI decreases with the increasing numbers of baffles and this may again be related to the observed improvement in the flow phenomena. Overall the curve fit was stable, as evidenced by the significant improvement in the goodness-of-fit statistics. The sum of squares due to error (SSE) decreased from **0.2064** to **0.1279** for the six and twelve baffle models respectively. Additionally, the root mean squared error (RMSE) decreased from **0.1703** to **0.0654**. The results of these statistical parameters indicate that the random component of error in the model is minimal and that it can be used as a prediction tool with reasonable confidence, provided the operating ranges are applicable. This can be further verified by performing a practical simulation at the given boundary conditions.

#### 4 CONCLUSIONS

In this study, a single pass TEMA E-type shell and tube heat exchanger was modelled in a steady state. The effects of turbulence on thermal performance were explored by varying turbulence level as a function of both mass flow and central baffle spacing for six, eight, ten, and twelve baffle models. The key finding was that decreasing baffle spacing improved the thermal performance at a cost of increased pressure drop. The CFD results were then combined with NLSQR to develop four sets of correlations relating Nu to Pr and Re. Given the reasonable goodness-of-fit parameters and confidence intervals the study reveals that the model can be used as a prediction tool with a reasonable level of confidence highlighting the potential of such workflows and integrations for practical design and optimization purposes. Further research work in the area needs to be conducted to explore the potential by improving the modelling schemes such as the grid quality and convergence tolerances, consideration of the flow in tube sides, flow conditions at inlet and outlets and the application of advanced prediction tools such as ANN (Artificial Neural Networks) to utilize the capability of decision making improving the potential and scope of thermal design and optimization. Another key improvement to judge the accuracy of the developed model would be to conduct practical simulations at the given boundary conditions.

#### REFERENCES

- Abbasi, H. R., Sharifi Sedeh, E., Pourrahmani, H., & Mohammadi, M. H. (2020). Shape optimization of segmental porous baffles for enhanced thermo-hydraulic performance of shell-and-tube heat exchanger. *Applied Thermal Engineering*, *180*, 115835. <https://doi.org/10.1016/j.applthermaleng.2020.115835>
- Alhulaifi, A. S. (2024). Computational Fluid Dynamics Heat Transfer Analysis of Double Pipe Heat Exchanger and Flow Characteristics Using Nanofluid TiO<sub>2</sub> with Water. *Designs*, *8*(3), 39. <https://doi.org/10.3390/designs8030039>
- Alperen, M. A., Kayabaşı, E., & Kurt, H. (2019). Detailed comparison of the methods used in the heat transfer coefficient and pressure loss calculation of shell side of shell and tube heat exchangers with the experimental results. *Energy Sources, Part A: Recovery, Utilization, and Environmental Effects*, 1–20. <https://doi.org/10.1080/15567036.2019.1672835>
- Aslam Bhutta, M. M., Hayat, N., Bashir, M. H., Khan, A. R., Ahmad, K. N., & Khan, S. (2012). CFD applications in various heat exchangers design: A review. *Applied Thermal Engineering*, *32*, 1–12. <https://doi.org/10.1016/j.applthermaleng.2011.09.001>
- Bichkar, P., Dandgaval, O., Dalvi, P., Godase, R., & Dey, T. (2018). Study of Shell and Tube Heat Exchanger with the Effect of Types of Baffles. *Procedia Manufacturing*, *20*, 195–200. <https://doi.org/10.1016/j.promfg.2018.02.028>
- El Maakoul, A., Laknizi, A., Saadeddine, S., El Metoui, M., Zaite, A., Meziane, M., & Ben Abdellah, A. (2016). Numerical comparison of shell-side performance for shell and tube heat exchangers with trefoil-hole, helical and segmental baffles. *Applied Thermal Engineering*, *109*, 175–185. <https://doi.org/10.1016/j.applthermaleng.2016.08.067>
- Huang, Z., Hwang, Y., & Radermacher, R. (2017). Review of nature-inspired heat exchanger

- technology. *International Journal of Refrigeration*, 78, 1–17. <https://doi.org/10.1016/j.ijrefrig.2017.03.006>
- Jamil, M. A., Goraya, T. S., Shahzad, M. W., & Zubair, S. M. (2020). Exergoeconomic optimization of a shell-and-tube heat exchanger. *Energy Conversion and Management*, 226, 113462. <https://doi.org/10.1016/j.enconman.2020.113462>
- M. Necati Özışık. (1985). *Heat Transfer*. McGraw-Hill Science, Engineering & Mathematics.
- Mangrulkar, C. K., Dhoble, A. S., Chamoli, S., Gupta, A., & Gawande, V. B. (2019). Recent advancement in heat transfer and fluid flow characteristics in cross flow heat exchangers. *Renewable and Sustainable Energy Reviews*, 113, 109220. <https://doi.org/10.1016/j.rser.2019.06.027>
- Marcinkowski, M., Dawid Taler, Katarzyna Węglarz, & Taler, J. (2024). Advancements in analyzing air-side heat transfer coefficient on the individual tube rows in finned heat exchangers: Comparative study of three CFD methods. *Energy*, 307, 132754–132754. <https://doi.org/10.1016/j.energy.2024.132754>
- Marcinkowski, M., Dawid Taler, Taler, J., & Katarzyna Węglarz. (2021). Thermal Calculations of Four-Row Plate-Fin and Tube Heat Exchanger Taking into Account Different Air-Side Correlations on Individual Rows of Tubes for Low Reynold Numbers. *Energies*, 14(21), 6978–6978. <https://doi.org/10.3390/en14216978>
- Nedunchezhiyan Mukilarasan, Karthikeyan, R., Ramalingam, S., Damodharan Dillikannan, Ravikumar, J., Sampath, S., & Gopal Kaliyaperumal. (2022). Influence of baffles in heat transfer fluid characteristics using CFD evaluation. *International Journal of Ambient Energy*, 43(1), 7088–7100. <https://doi.org/10.1080/01430750.2022.2063175>
- Ozden, E., & Tari, I. (2010). Shell side CFD analysis of a small shell-and-tube heat exchanger. *Energy Conversion and Management*, 51(5), 1004–1014. <https://doi.org/10.1016/j.enconman.2009.12.003>
- Pal, E., Kumar, I., Joshi, J. B., & Maheshwari, N. K. (2016). CFD simulations of shell-side flow in a shell-and-tube type heat exchanger with and without baffles. *Chemical Engineering Science*, 143, 314–340. <https://doi.org/10.1016/j.ces.2016.01.011>
- Sauro, J., & Lewis, J. R. (2012). How Precise Are Our Estimates? Confidence Intervals. *Quantifying the User Experience*, 19–39. <https://doi.org/10.1016/b978-0-12-384968-7.00003-5>
- Sekulić, D. P., & Shah, R. K. (2023). *Fundamentals of Heat Exchanger Design*. Wiley. <https://doi.org/10.1002/9781119883296>
- Shahril, S. M., Quadir, G. A., Amin, N. A. M., & Badruddin, I. A. (2017). Thermo hydraulic performance analysis of a shell-and-double concentric tube heat exchanger using CFD. *International Journal of Heat and Mass Transfer*, 105, 781–798. <https://doi.org/10.1016/j.ijheatmasstransfer.2016.10.021>
- Zhang, X., Han, D., He, W., Yue, C., & Pu, W. (2017). Numerical simulation on a novel shell-and-tube heat exchanger with screw cinquefoil orifice baffles. *Advances in Mechanical Engineering*, 9(8), 168781401771766–168781401771766. <https://doi.org/10.1177/1687814017717665>